

# ansa-Metallocene-Based Cyclic[2]pyrroles

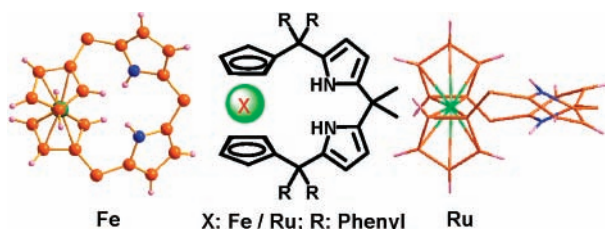
S. Ramakrishnan and Alagar Srinivasan\*

Photosciences and Photonics Section, Chemical Sciences and Technology Division,  
National Institute for Interdisciplinary Science and Technology (NIIST-CSIR),  
Thiruvananthapuram 695 019, Kerala, India

indiansrini@gmail.com

Received August 22, 2007

## ABSTRACT



Syntheses and X-ray structural analyses of *ansa*-metallocene-based cyclic[2]pyrroles are described. The pyrrole units in the macrocycles adopt partial 1,2-alternate conformation in the solid state.

The development of receptors for recognizing cation, anion, and neutral species has attracted much attention in molecular recognition study and supramolecular chemistry.<sup>1</sup> One class of receptors is organic based, examples of which consist of polyammonium-based receptors,<sup>2a</sup> guanidium-based receptors,<sup>2b</sup> bipyrrrole catenanes,<sup>2c</sup> expanded porphyrins,<sup>2d</sup> dipyrrolylquinoxalines,<sup>2e</sup> calixpyrroles,<sup>2f</sup> amidopyrrole clefts,<sup>2g</sup> and pyrrole–diketo derivatives.<sup>2h</sup> The other class of receptors are inorganic based which offer a number of advantages over the organic counterparts. For example, metal ions often display redox activity, UV–vis spectroscopic properties, and fluorescent and energy transfer properties, all of which can allow for a measurement of the anion-binding event. Examples of inorganic receptors include those containing Lewis acid metals such as Sn, B, Si, Ge, or Hg as well as multiple positively charged metal ion based receptors.<sup>3</sup>

More germane to the current work are anion receptors containing redox groups that are covalently or noncovalently linked to the receptor moieties. These electrochemical responsive receptors are widely suitable in the areas of chemical sensors, redox catalysts, and redox-switchable ligands.<sup>4</sup> The use of metallocenes, particularly, ferrocene and ruthenocene, as an electrochemically active “reporter group” has been explored by a number of research groups.<sup>5</sup> Currently, there are numerous examples of macrocycles in which ferrocenes are externally appended to various anion-

(1) (a) Beer, P. D.; Gale, P. A. *Angew. Chem., Int. Ed.* **2001**, *40*, 486. (b) Martínez-Máñez, R.; Sancenón, F. *Chem. Rev.* **2003**, *103*, 4419. (c) Sessler, J. L.; Camiolo, S.; Gale, P. *Coord. Chem Rev.* **2003**, *240*, 17.

(2) (a) García-España, E.; Díaz, P.; Llinares, J. M.; Bianchi, A. *Coord. Chem. Rev.* **2006**, *250*, 2952. (b) Schmuck, C.; Lex, J. *Eur. J. Org. Chem.* **2001**, 1519. (c) Andrievsky, A.; Ahuis, F.; Sessler, J. L.; Vögtle, F.; Gudat, G.; Moini, M. *J. Am. Chem. Soc.* **1998**, *120*, 9712. (d) Sessler, J. L.; Davis, J. *Acc. Chem. Res.* **2001**, *34*, 989. (e) Black, C. B.; Andrioletti, B.; Try, A. C.; Rupierez, C.; Sessler, J. L. *J. Am. Chem. Soc.* **1999**, *121*, 10438. (f) Gale, P. A.; Sessler, J. L.; Král, V.; Lynch, V. *J. Am. Chem. Soc.* **1996**, *118*, 5140. (g) Gale, P. A.; Quesada, R. *Coord. Chem. Rev.* **2006**, *250*, 3219. (h) Maeda, H.; Kusunose, Y. *Chem. Eur. J.* **2005**, *11*, 5661.

(3) (a) Azuma, Y.; Newcomb, M. *Organometallics* **1984**, *3*, 9. (b) Reetz, M. T.; Niemeyer, C. M.; Harms, K. *Angew. Chem., Int. Ed. Engl.* **1991**, *30*, 1472. (c) Tamao, K.; Hayashi, T.; Ito, Y. *J. Organomet. Chem.* **1996**, *506*, 85. (d) Aoyagi, S.; Ogawa, K.; Tanaka, K.; Takeuchi, Y. *J. Chem. Soc., Perkin Trans. 2* **1995**, 355. (e) Zheng, Z.; Yang, X.; Knobler, C. B.; Hawthorne, M. F. *J. Am. Chem. Soc.* **1991**, *115*, 5320.

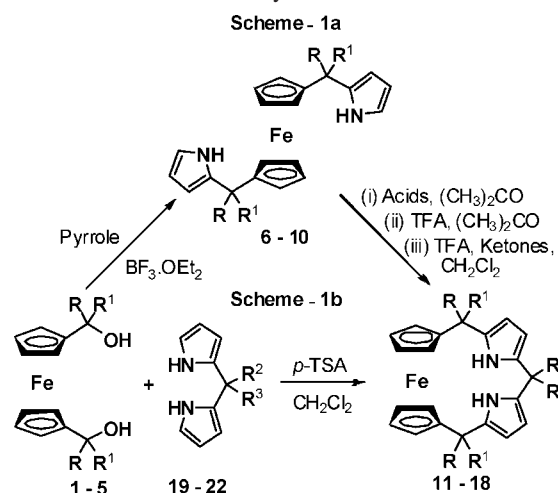
(4) (a) Gale, P. A. *Coord. Chem. Rev.* **2000**, *199*, 181. (b) Tendero, M. J. L.; Benito, A.; Cano, J.; Lloris, J. M.; Martínez-Máñez, R.; Soto, J.; Edwards, A. J.; Raithby, P. R.; Rennie, A. *J. Chem. Soc., Chem. Commun.* **1995**, 1643. (c) Kaifer, A. E.; Mendoza, S. In *Comprehensive Supramolecular Chemistry*; Gokel, G. W., Ed.; Pergamon: Oxford, 1996; Vol. 1.

(5) (a) Reynes, O.; Bucher, C.; Mouter, J.-C.; Royal, G.; Aman, E. S.; Ungureanu, E.-M. *J. Electroanal. Chem.* **2005**, *580*, 291. (b) Otón, F.; Tórraga, A.; Espinosa, A.; Velasco, M. D.; Molina, P. *J. Org. Chem.* **2006**, *71*, 4590. (c) Tomapatanaget, B.; Tuntulani, T.; Chailapakul, O. *Org. Lett.* **2003**, *5*, 1539. (d) Beer, P. D.; Gale, P. A.; Chen, G. Z. *J. Chem. Soc., Dalton Trans.* **1999**, 1897. (e) Collinson, S. R.; Gelbrich, T.; Hursthouse, M. B.; Tucker, J. H. R. *Chem. Commun.* **2001**, 555. (f) Plenio, H.; Aberle, C. *Angew. Chem., Int. Ed.* **1998**, *37*, 1397. (g) Beer, P. D.; Cadman, J. *Coord. Chem. Rev.* **2000**, *205*, 131.

binding porphyrin or porphyrin analogue receptors, and calixpyrroles are discussed.<sup>6</sup> Recently, Sessler has reported *ansa*-ferrocene type bridged pyrrolic systems that show significant perturbations in their electrochemical properties in the presence of anionic guests.<sup>7</sup> However, incorporating metallocene into the backbone of calixpyrrole systems in an *ansa*-type way is not known. Herein, we wish to report the synthesis of the *ansa*-ferrocene-based cyclic[2]pyrroles. Similar chemistry is further extended into *ansa*-ruthenocene moiety.

The precursors for the target macrocycles **11–18**, such as diols **1–5**, are synthesized from the reaction of a 1,1'-bis-lithiated salt of ferrocene with various ketones in 20–80% yield (Scheme 1, route a), respectively.<sup>8</sup> The hitherto

Scheme 1. Synthesis of **11–18**



unknown 1,1'-ferrocenylbis(*gem*-dialkyl/diaryl/cyclohexyl/alkylaryl)dipyrromethanes (**6–10**) are obtained by the BF<sub>3</sub>·OEt<sub>2</sub>-catalyzed condensation of pyrrole and diol (**1–5**) in 65–80% yield (Table 1). The synthetic methodology adopted here is entirely different from the work reported by Sessler and co-workers, where they generated the 1,1'-ferrocenyl-dipyrromethane from the isomeric mixture of cyclopentadienyl-functionalized pyrroles.<sup>7a</sup>

The FAB mass spectral analysis of **1–10** predicted the exact composition of the starting materials. The <sup>1</sup>H NMR analysis of **6–10** shows signals corresponding to half the linear chain, suggesting the symmetrical nature in which the pyrrole rings are opposite to each other. This is further confirmed by single-crystal X-ray analysis of **6** as shown in

(6) (a) Beer, P. D. *Chem. Commun.* **1996**, 689. (b) Beer, P. D.; Drew, M. G. B.; Jagessar, R. J. *Chem. Soc., Dalton Trans.* **1997**, 881. (c) Sessler, J. L.; Gebauer, A.; Gale, P. A. *Gazz. Chim. Ital.* **1997**, 127, 723. (d) Gale, P. A.; Hursthouse, M. B.; Light, M. E.; Sessler, J. L.; Warriner, C. N.; Zimmerman, R. S. *Tetrahedron Lett.* **2001**, 45, 6759. (e) Bucher, C.; Zimmerman, R. S.; Lynch, V.; Král, V.; Sessler, J. L. *J. Am. Chem. Soc.* **2001**, 123, 2099.

(7) (a) Scherer, M.; Sessler, J. L.; Gebauer, A.; Lynch, V. *Chem. Commun.* **1998**, 85. (b) Sessler, J. L.; Zimmerman, R. S.; Kirkovits, G. J.; Gebauer, A.; Scherer, M. J. *Organomet. Chem.* **2001**, 637–639, 343.

(8) Carroll, M. A.; Widdowson, D. A.; Williams, D. J. *Synlett* **1994**, 1025.

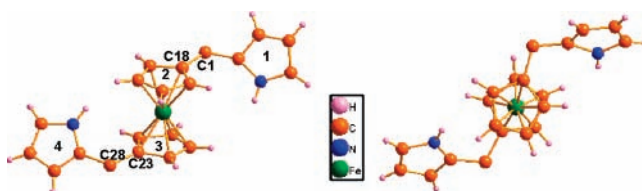
Table 1. Yields of **1–18**

no.	R	R <sup>1</sup>	yield (%)	acids	<b>11</b> (%)
<b>1</b> ( <b>6</b> )	C <sub>6</sub> H <sub>5</sub>	C <sub>6</sub> H <sub>5</sub>	80 (80)	BF <sub>3</sub> ·OEt <sub>2</sub>	25
<b>2</b> ( <b>7</b> )	CH <sub>3</sub>	C <sub>6</sub> H <sub>5</sub>	26 (65)	SnCl <sub>4</sub>	28
<b>3</b> ( <b>8</b> )	cyclohexyl		20 (80)	TFA	48
<b>4</b> ( <b>9</b> )	C <sub>2</sub> H <sub>5</sub>	C <sub>2</sub> H <sub>5</sub>	21 (68)	<i>p</i> -TSA	46
<b>5</b> ( <b>10</b> )	CH <sub>3</sub>	CH <sub>3</sub>	23 (65)	MSA	41

no.	R	R <sup>1</sup>	R <sup>2</sup>	R <sup>3</sup>	yield (%)	
					Scheme 1, route a <sup>a</sup>	Scheme 1, route b
<b>11</b>	C <sub>6</sub> H <sub>5</sub>	C <sub>6</sub> H <sub>5</sub>	CH <sub>3</sub>	CH <sub>3</sub>	48	23
<b>12</b>	CH <sub>3</sub>	C <sub>6</sub> H <sub>5</sub>	CH <sub>3</sub>	CH <sub>3</sub>	19	18
<b>13</b>	cyclohexyl		CH <sub>3</sub>	CH <sub>3</sub>	22	20
<b>14</b>	C <sub>2</sub> H <sub>5</sub>	C <sub>2</sub> H <sub>5</sub>	CH <sub>3</sub>	CH <sub>3</sub>	19	17
<b>15</b>	CH <sub>3</sub>	CH <sub>3</sub>	CH <sub>3</sub>	CH <sub>3</sub>	25	22
<b>16</b>	CH <sub>3</sub>	C <sub>6</sub> H <sub>5</sub>	CH <sub>3</sub>	C <sub>6</sub> H <sub>5</sub>	23	19
<b>17</b>	cyclohexyl		cyclohexyl		25	22
<b>18</b>	C <sub>2</sub> H <sub>5</sub>	C <sub>2</sub> H <sub>5</sub>	C <sub>2</sub> H <sub>5</sub>	C <sub>2</sub> H <sub>5</sub>	17	16

<sup>a</sup> In Scheme 1, route a, **11–15** were synthesized under the reaction conditions (ii), while **16–18** were synthesized via (iii).

Figure 1.<sup>9a</sup> The structure clearly shows that the pyrrole rings are trans to each other with respect to the ferrocene ring and



showing that the molecule adopts a helical twist in the solid state. This twisting of the molecule avoids the formation of linear polymeric products during the condensation process, thus supporting the so-called helical effect involved in the formation of the macrocycles.<sup>10</sup>

The syntheses of **11**–**18** are shown in Scheme 1, routes a and b, and the yields are mentioned in Table 1. In Scheme 1, route a, we used three different reaction conditions: (i) varying the acid catalyst, (ii) using acetone as solvent as well as reactant, and (iii) mixing various ketones in CH<sub>2</sub>Cl<sub>2</sub> solvent. The suitable acid catalyst is identified from (i) and used as such in (ii) and (iii). Initially, in (i), we concentrated mainly on the synthesis of **11** by using 0.1 equiv of various catalysts such as Lewis to protic acids. Thus, acid-catalyzed condensation of **6** with acetone (30 mL) afforded **11**, and the observed yields are shown in Table 1. The yield was found to be dependent on the nature of the acid catalyst used. The lower yield of **11** in the presence of Lewis acid indicates the partial acidolysis of **6**. Evidence of the acidolysis has come from the following observation, where the TLC (silica gel G; ethyl acetate/hexane 1:25) analysis of **6** with 0.1 equiv of BF<sub>3</sub>·OEt<sub>2</sub> indicated a decrease in the concentration of the **6**. A similar trend was observed by Lindsey and co-workers, wherein the dipyrromethanes undergo partial acidolysis depending on the Lewis acid concentration and nature of the meso substituents.<sup>11</sup>

Overall, TFA was found to be well suited in (i) and employed for the syntheses of remaining macrocycles **12**–**18**. Thus, by using condition (ii), a series of 1,1'-ferrocenyl-substituted dipyrromethanes (**7**–**10**) reacted with acetone in the presence of catalyst afforded **12**–**15** in 19–25% yield, respectively. On the other hand, in (iii), by using 30 mL of CH<sub>2</sub>Cl<sub>2</sub>, similar ketones, which are used for the synthesis of **2**–**4**, are condensed with the respective dipyrromethanes (**7**–**9**) under identical reaction conditions to give **16**–**18** in 17–25% yield, respectively (Table 1). Both conditions mentioned here are straightforward with no side-product formation. However, we observed a trace amount of two more products along with **15**. The FAB mass analysis of the new products suggested the formation of the expanded derivatives of **15**.<sup>12</sup>

In order to improve the yields of **11**–**18**, we adopted a different synthetic route, which is shown in Scheme 1, route b. *p*-Toluenesulfonic acid-catalyzed condensation of 1,1'-ferrocenediol with a series of dipyrromethanes (**19**–**22**)<sup>11</sup> afforded **11**–**18** in 16–23% yield, respectively. However, the obtained yields are comparable to those in Scheme 1, route a. Thus, varying the synthetic methodology did not alter the yield of the macrocycle formation.

The exact compositions of the macrocycles were confirmed by the FAB mass spectral analysis. The <sup>1</sup>H, <sup>13</sup>C NMR spectral

analyses of all the precursors and macrocycles and <sup>1</sup>H–<sup>1</sup>H COSY spectrum of **11** were recorded at room temperature in CDCl<sub>3</sub>.<sup>13</sup>

As a representative example, the <sup>1</sup>H NMR spectra of **11** and **15** are shown in Figure 2. The NH protons of **11** and **15**

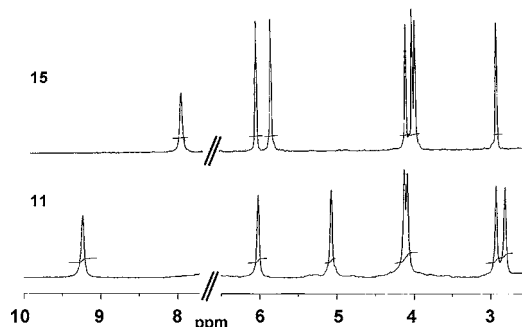


**Figure 2.** <sup>1</sup>H NMR spectra of **11** and **15**. The signals correspond to the protons of the meso groups, and the signals of CDCl<sub>3</sub> are omitted for clarity.

resonate at 9.24 and 7.88 ppm, while the pyrrolic β-CH and ferrocenyl-CH protons resonate between 2.5 and 7.0 ppm, respectively. This suggested that NH protons in **11** are shifted downfield (1.36 ppm), while the pyrrolic β-CH and ferrocenyl-CH protons are 0.37 ppm upfield shifted as compared to **15**. The D<sub>2</sub>O-exchangeable signals at 9.24 and 7.88 (**11** and **15**) ppm assigns the NH protons. Further, the absence of two α-CH protons in the pyrrolic rings, which are observed in **6**, proved by <sup>1</sup>H and <sup>1</sup>H – <sup>1</sup>H COSY spectral analysis of **11**, where the correlation between the pyrrolic NH with β-CH protons suggests the formation of the macrocycle.<sup>13</sup> In addition, compared to the linear chains **6** – **10**, the pyrrolic β-CH and ferrocenyl-CH protons in **11** – **18** are upfield shifted with the shift difference of 0.05 to 0.53 ppm, further supported the macrocyclic ring formation.<sup>13</sup>

The confirmation of the proposed structure came from the single-crystal X-ray analysis of **11** as shown in Figure 3.<sup>9b</sup> As suggested from the above observations, the pyrrole units are connected to the ferrocenyl rings through the *meso*-carbon bridges. The dihedral angles between the two planes (1 and 2; 3 and 4) in **11** are 68.43 and 68.37°, respectively. The pyrrole rings (1 and 4) in **6** rotate in clockwise and anticlockwise directions with angles of 11.96 and 18.47° and condense with acetone in the presence of acid catalyst to form the macrocycle **11**. This is achieved through the single bond rotation in **6** between C1–C18 and C23–C28. Further, the side view shows that both the pyrrole rings in the macrocycle adopts partial 1,2-alternate conformation in the solid state. The dihedral angle between the two planes is (1 and 4) 46.27° and the distance between the two pyrrole units is 4.45 Å. It is pertinent to point out here that the parent

(10) (a) Sessler, J. L.; Weghorn, S. J.; Hiseada, Y.; Lynch, V. *Chem. – Eur. J.* **1995**, *1*, 56. (b) Franck, B. *Angew. Chem., Int. Ed. Engl.* **1982**, *21*, 343. (c) Tietze, L. F.; Geissler, H. *Angew. Chem., Int. Ed. Engl.* **1993**, *32*, 1040.

(11) Lee, C.-H.; Lindsey, J. S. *Tetrahedron* **1994**, *50*, 11427. In **19**, R<sup>2</sup> = R<sup>3</sup> = CH<sub>3</sub>; **20**, R<sup>2</sup> = CH<sub>3</sub>, R<sup>3</sup> = C<sub>6</sub>H<sub>5</sub>; **21**, R<sup>2</sup> = R<sup>3</sup> = cyclohexyl; **22**, R<sup>2</sup> = R<sup>3</sup> = C<sub>2</sub>H<sub>5</sub>.

(12) FAB mass showed the molecular ion peak at *m/z* = 880.19 [M<sup>+</sup>] and 1321.03 [M + 1] suggested the formation of 2:2 and 3:3 macrocycles (ferrocene dipyrromethane/acetone).

(13) See the Supporting Information: Figure 8 and Table 1.

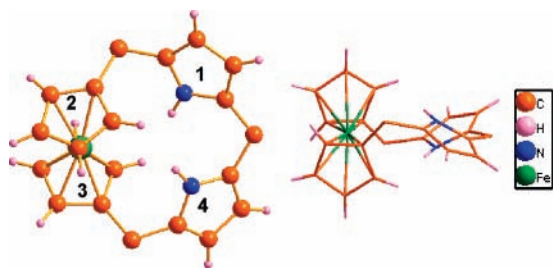
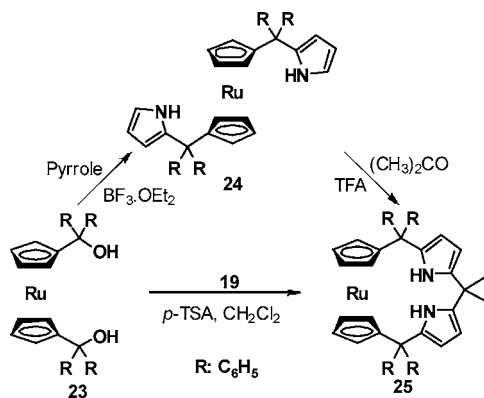


**Figure 3.** X-ray structure of **11**. The meso groups are omitted for clarity in the top and side view.

compound, calix[4]pyrrole, adopts a 1,2-alternate conformation in the solid state.<sup>2f</sup>

The chemistry is further extended into the next higher metallocene, such as, ruthenocene. The diol (**23**) is achieved from the 1,1'-bis-lithiated salt of ruthenocene and benzophenone with a yield of 68%. Compound **23** is condensed with pyrrole in the presence of  $\text{BF}_3 \cdot \text{OEt}_2$  to form the dipyrromethane **24** in 81% yield. The *ansa*-ruthenocene-based cyclic[2]pyrroles (**25**) are synthesized by the TFA acid-catalyzed condensation of **24** with acetone as solvent as well as reactant, affording **25** in 24% yield. Alternatively, **25** was synthesized by condensing **19** with **23** in the presence of *p*-TSA in 21% yield (Scheme 2).

**Scheme 2.** Synthesis of **25**



The  $^1\text{H}$  NMR analysis of **25** shows the pyrrolic NH,  $\beta$ -CH and ferrocenyl CH protons at 8.86, 5.57, and 3.98 ppm, respectively. As in **11**, a similar trend is observed in **25**,

where the pyrrolic  $\beta$ -CH and ferrocenyl CH protons are upfield shifted, as compared to **24**, with the shift difference of 0.27 and 0.34 ppm, respectively.<sup>13</sup> The macrocyclic ring formation is further confirmed by single-crystal X-ray analysis of **25**, where the dihedral angle between the two pyrrolic rings (plane 1 and 2) is  $45.96^\circ$  with a distance of  $4.48(3) \text{ \AA}$ , respectively.<sup>9c</sup> The side view further confirms that the pyrrole rings in **25** maintains a 1,2-alternate conformation in the solid state (Figure 4).

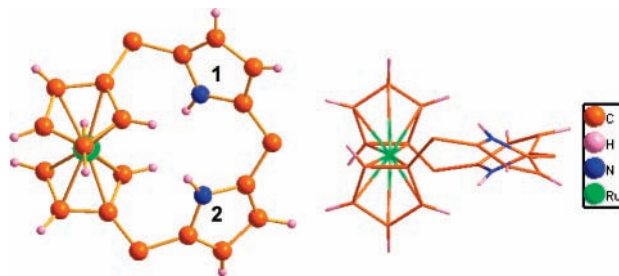


**Figure 4.** X-ray structure of **25**. The meso groups are omitted for clarity in the top and side view.

In conclusion, we have demonstrated the syntheses of *ansa*-metallocene-based cyclic[2]pyrroles. For the first time, metallocene units are incorporated into the backbone of the calixpyrrole frame work. The partial 1,2-alternate conformation in the solid state proved that the macrocycle retains the calixpyrrole behavior. The synthetic methodology is simple and straightforward due to the absence of side products and easier purification. Efforts are currently underway to explore the anion binding properties of these macrocycles and also the synthesis of respective calixphyrin, porphyrin, and expanded calixpyrrole derivatives.

**Acknowledgment.** Dr. A.S. thanks DST, New Delhi, and the Director, NIIST-CSIR, for financial support. S.R.K. thanks UGC for the fellowship. We thank Dr. Babu Varghese and Dr. Moni, SAIF, IIT-Chennai, for solving the crystal structure and recording the  $^{13}\text{C}$  NMR spectra. We greatly acknowledge Mrs. Viji, Sowmini, and Mr. Deepak, NIIST, CSIR, for recording the FAB, NMR, and IR spectra.

**Supporting Information Available:** Synthetic procedures, melting point, and IR,  $^1\text{H}$ ,  $^{13}\text{C}$ , and FAB mass spectral data for all new compounds. Crystal data for **6**, **11**, and **25** (CIF). This material is available free of charge via the Internet at <http://pubs.acs.org>.

OL702021K